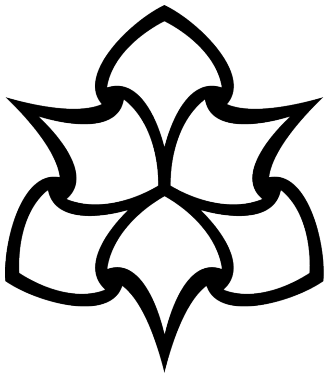

Label-free protein detection based on the heat-transfer method – a case study with the peanut allergen Ara h 1 and aptamer-based synthetic receptors

Marloes Peeters [1,2,*], Bart van Grinsven [3], Thomas J. Cleij [3], Kathia Lorena Jiménez-Monroy [1], Peter Cornelis [4], Elena Pérez-Ruiz [6], Gideon Wackers [1,4], Ronald Thoelen [1,5], Ward De Ceuninck[1,5], Jeroen Lammertyn [6], and Patrick Wagner [1,4]

1) Hasselt University, Institute for Materials Research, Wetenschapspark 1, 3590 Diepenbeek, Belgium

2) Queen Mary University of London, School of Biological and Chemical Sciences, Mile End Road, London E1 4NS, United Kingdom

3) Maastricht University, Maastricht Science Programme, P.O. Box 616, 6200 MD Maastricht, the Netherlands

4) Catholic University Leuven, Department of Physics and Astronomy, Soft-Matter and Biophysics Section, Celestijnenlaan 200 D, 3001 Leuven, Belgium

5) IMEC v.z.w. division IMOMEC, Wetenschapspark 1, 3590 Diepenbeek, Belgium

6) KU Leuven – University of Leuven BIOSYST-MeBioS, Willem de Crooylaan 42, 3000 Leuven, Belgium

Abstract: Aptamers are an emerging class of molecules which, due to the development of the systematic evolution of ligands by exponential enrichment (SELEX) process, can recognize virtually every target ranging from ions, to proteins, and even whole cells. While there are many techniques capable of detecting template molecules with aptamer-based systems with high specificity and selectivity, they lack the possibility of integrating them into a compact and portable biosensor setup. Therefore, we will present the heat-transfer method (HTM) as an interesting alternative since this offers detection in a fast and low-cost manner and has the possibility of performing experiments with a fully integrated device. This concept has been demonstrated for a variety of applications including DNA mutation analysis and screening of cancer cells. To our knowledge, this is the first report on HTM-based detection of proteins, in this case specifically with aptamer-type receptors. For proof-of-principle purposes, measurements will be performed with the peanut allergen Ara h 1 and results indicate detection limits in the lower nanomolar regime in buffer liquid. As a first proof-of-application, spiked Ara h 1 solutions will be studied in a food matrix of dissolved peanut butter. Reference experiments with the quartz-crystal microbalance will allow for an estimate of the areal density of aptamer molecules on the sensor-chip surface.

Keywords: label-free biosensors, biomimetic sensors, heat-transfer method (HTM), aptamers, proteins, Ara h 1.

Corresponding author*: Dr. Marloes Peeters
Queen Mary University of London
School of Biological and Chemical Sciences
Mile End Road
London E1 4NS
United Kingdom

Phone: + 44 – 20 – 78 82 33 20
E-mail: m.peeters@qmul.ac.uk

1. Introduction

Aptamers are synthetic oligonucleotides which can specifically bind target molecules based on a combination of hydrogen bonding, electrostatic interactions, van der Waals forces and their three dimensional conformation[1,2]. The selection of the optimal aptamer for a given target molecule is accomplished *in vitro via* a SELEX process (Systematic Evolutions of Ligands by EXponential enrichment) from libraries containing random oligonucleotide sequences[3,4]. With this procedure, it is possible to develop aptamers for a variety of target categories ranging from ions[5], to proteins[6,7], and even to whole cells[8,9]. Aptasensors have already been designed based on capillary electrophoresis[10], colorimetric assays[11], fluorescence anisotropy[12], surface plasmon resonance[13], and microgravimetric sensing[14]. These techniques ensure a high specificity and selectivity; however they are less suited for integration into portable, low-cost sensor devices. In that aspect, field-effect transducers and electrochemical impedance spectroscopy are interesting alternatives[15,16,17]. Tran *et al.* described an aptamer-based, impedimetric sensor platform which could specifically detect IgE in buffer solutions and human serum samples[18]. These measurements were performed with a high-end impedance analyzer requiring comparatively long measurement times and a refined data analysis based on the phase angle of the impedance signal. More recently, Peeters *et al.* developed an aptamer-based, impedimetric sensor system in pocket format, allowing detecting the peanut allergen Ara h 1 specifically and quantitatively correct in the lower nanomolar regime in buffers[19]. The sensor output in this case was simply the amplitude of the impedance signal at a given frequency. While impedimetric measurements allow for a considerable system miniaturization, data acquisition and processing still require a piece of software- and hardware engineering.

Within in this article, we will therefore present an aptasensor based on a purely thermometric concept, the heat-transfer method (HTM). This technique has the benefits of being straightforward and requiring only limited hardware, merely two temperature sensors and a heat-source that can be regulated to keep a pre-defined temperature. This is analogous to a *dc* resistivity measurement in which the electronic current is replaced by a thermal current. Until date, this method has been applied successfully for the analysis of DNA mutations[20,21], detection of cells and small organic molecules[22,23], and phase transitions in lipids[24], but not yet in the context of proteins. The latter is considered as one of the most challenging tasks in label-free biosensing and it is *a priori* unclear whether the recognition of proteins by aptamers brings about measurable changes of the heat-transfer resistance. We

point out that the HTM principle is conceptually different from the approach by Wang *et al.* who detected thrombin with aptamers by determining the binding enthalpy calorimetrically in a sandwich-type assay with detection limits down to 22 nM[25]. In contrast to this, HTM aims at the detection of molecules from the heat-transfer resistance under steady-state conditions and does not necessitate a temperature ramping of the sample under study.

Until now, the heat-transfer principle is based on empirical grounds and the theoretical foundations are not yet developed. However, there is clearly an interest for heat transport through biological molecules as illustrated *e.g.* by the vibrational-dynamics studies on double- and single-stranded DNA molecules[26] and the molecular dynamics simulations of heat flow through lipid membranes[27]. As a possible starting point for a deeper understanding of the principle behind the HTM technique we note that all aforementioned applications have a common denominator: The enhancement of the heat-transfer resistance goes along with a structural softening at the solid (sensor chip) to liquid interface. In case of DNA this is the transition from 'rigid' double-stranded DNA to highly flexible single-stranded DNA[21]. In case of cell recognition by surface imprints, mechanically flexible membrane material adheres to the polymeric surface[28]. A jump-like R_{th} increase is observed when lipid vesicles undergo their main phase transition from the gel- to the liquid-disordered phase[24]. Finally, the small-molecule recognition by molecularly imprinted polymers is based on the weak and reversible binding of these molecules in molecular-size cavities. In summary, these are interface effects in which the molecular layer right at the interface is gaining additional degrees of freedom. Regarding aptamers, we will address below whether the capturing of proteins is also associated with gaining additional degrees of freedom at the solid-to-liquid interface. Throughout all experiments described below, *i.e.* before, during and after capturing of the target proteins, the aptamers are in their natural, temperature- and pH-dependent conformation without utilizing neutralizing oligomers: This concept, introduced recently by Das and coworkers, forces aptamers into a straight and rigid configuration before binding of the molecular targets and seems beneficial for achieving ultralow detection limits when combined with a fluorescence-based readout system[29].

For proof-of-principle purposes, we will first show the HTM-based thermal detection of Ara h 1 in buffer solutions with an aptamer-based sensor platform. This system was selected for two reasons: First, the molecular recognition between the aptamer and Ara h 1 has already been thoroughly studied[30] and, second, it is highly relevant for the food industry as the peanut allergen Ara h 1 (a trimeric protein with 195 kDa molecular weight) is responsible for most

food-related anaphylactic shocks[18]. To demonstrate the principle not only in buffer solutions but to provide also a first proof-of-application, experiments will be performed with spiked Ara h 1 samples in a matrix enriched with peanut butter. The sensor platform is generic, making it probably possible to detect a variety of other proteins with only minor modifications, provided that corresponding aptamers do exist. In summary, this is the first sensor platform based on the thermal HTM read-out technique, which can detect proteins in buffers and, moreover, also in more complex matrices. This illustrates that also the molecular recognition of a protein by an aptamer goes along with a measurable heat-transfer effect.

2. Experimental

2.1 Materials

The thiol 11-mercapto-undecanoic acid (MUA) and bovine serum albumin (BSA, $M_r \sim 66.5$ kDa) were purchased from Sigma Aldrich (Steinheim, Germany) and 1-ethyl-3-(3-dimethyl-aminopropyl)carbodiimide (EDC) from Thermo Scientific (Aalst, Belgium). The peanut allergen Ara h 1 was obtained from INDOOR technologies (Cardiff, Wales) and used as received. The compounds required for the preparation of the buffers, respectively, 2-(N-morpholino)ethanesul-fonic acid (MES buffer, pH 6.0), tris(hydroxyamino)methane-glycine-potassium (TGK buffer, pH 8.3) and phosphate buffered saline solution (PBS buffer, pH 7.4), were purchased from Sigma Aldrich (Steinheim, Germany) and Fisher Scientific (Landsmeer, the Netherlands). Ethanol of analytical grade (anhydrous, purity 99.9%) was from VWR (Leuven, Belgium). The optimal aptamer for Ara h 1 detection had been determined in previous research by Tran *et al.* and the sequence is given below[13].

Aptamer sequence: $NH_2 - C_6 - 5'$
TCGCACATTCCGCTTCTACCGGGGGGGTCGAGCTGAGTGGATGCGAATCTGTGGG
TGGGCCGTAAGTCCGTGTGTGCGAA 3'

This sequence, consisting of 80 nucleotide bases, was ordered from IDT Technologies (Leuven, Belgium). The 5' end, serving for attachment to the thiols, was modified with an amino group and a C_6 carbon spacer. The structural conformation of the aptamer at selected temperatures, calculated with the online software package 'Mfold' [31], can be found in ref[18]. As shown previously, this optimized Ara-h1 aptamer shows negligible cross selectivity to proteins with a similar molecular weight such as horse-radish peroxidase (HRP) and BSA[19].

Even more importantly, reference tests with a second important peanut allergen, Ara h 2 with 17 kDa, have proven negative[13].

2.2 Aptamer functionalization of sensor chips and protein-sample preparation

The sensor chips, see **Figure 1** for a schematic layout, consisted of gilded silicon substrates (1 $\times$ 1 cm^2, 450 µm thickness) which were prepared as follows: First, a 20 nm adhesive layer of chromium was thermally evaporated under a vacuum pressure of 5×10^{-5} Pa onto doped silicon chips, followed then by a 80 nm layer of gold. These chips were treated with a Digital PSD series UV-ozone system from Novoscan (Nürnberg, Germany) for 1 h in order to clean the surface and make them more hydrophilic by surface-bound oxygen species. Subsequently, they were briefly exposed to a cold "piranha" solution (H_2O_2 and H_2SO_4 in a 1:3 ratio), rinsed with ethanol, and then incubated for 48 h with a MUA thiol solution in ethanol (concentration 1 mM) at room temperature under nitrogen atmosphere. After cleaning the samples in pure ethanol, the amino-terminated Ara h 1 aptamers were attached via direct EDC coupling in MES buffer of pH 6. This process was monitored *in-real time* by probing the thermal resistance at the solid-liquid interface. In order to reduce non-specific adsorption, especially of proteins, the aptamer-functionalized gold surface was blocked by immersing the substrates overnight into a BSA solution (50 nM in PBS, temperature of 4 ^{0}C), generating a blocking BSA monolayer[18].

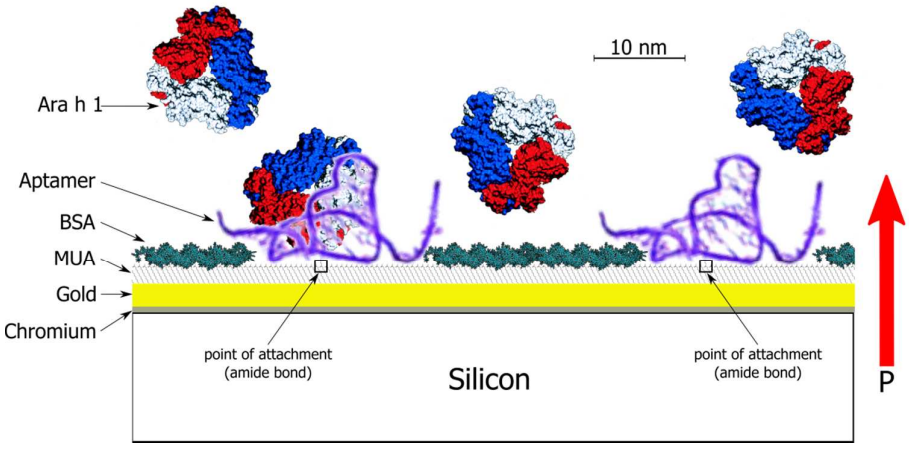

Figure 1: Scheme of the sensor-chip layout in which the amino-modified aptamer is EDC-coupled to a self-assembled monolayer of MUA thiols on gold. The BSA overcoating serves for blocking non-specific adsorption. Under the chosen conditions (TGK buffer with pH 8.3, 37 ^{0}C) the aptamer is expected to attain the indicated conformation before binding of the Ara

h 1 antigen. The flow direction of the heating power P is indicated. The aptamer, BSA, and Ara h 1 are drawn to scale, the scale bar indicates 10 nm[32,33].

The aptasensor was now ready for use and, after stabilizing in TGK buffer, various solutions of Ara h 1 concentrations (5, 10, 15, 25, and 50 nM) in TGK buffer were added sequentially to the set up. To address the specificity of the molecular recognition, reference experiments were also performed with a chip with only the SAM and its BSA overcoating, but without presence of the aptamer. As a first proof-of-application, measurements were performed in a matrix enriched with peanut butter. To obtain these samples, 50 mg of peanut butter (Unilever – Calvé , Delft, the Netherlands) was first molten and then dissolved into 200 ml of TGK buffer by stirring for 2 hours at 50 ^{0}C. After filtration through a filter with 1 micron pore size, the resulting fluid (also addressed as 'buffer diluted extract') was split into two aliquots one of which was unaltered and the other one spiked with 100 nM of Ara h 1. The concentration of Ara h 1 in the non-spiked, buffer-diluted extract can be estimated as follows: The amount of 25 mg peanut butter per 100 ml equals 20 mg of pure peanut substance, corresponding to 5 mg of proteins. According to literature, the maximum percentage of Ara h 1 in the total protein contents is 16% [34,35], meaning that there is maximal 0.8 mg of Ara h 1 present in the 100 ml of extract. Together with the molecular mass of Ara h 1 (195 kDa) this corresponds to an upper limit of the Ara h 1 concentration of 40 nM.

2.3 *The thermal resistance set up*

The equipment used for the thermal resistance measurements was an in-house design, see Figure 2, which was described previously in detail in ref[20]. A schematic drawing with the exact dimensions of the equipment can be found in Figure S-1 of the Supporting Information. To this system, a Perspex flow cell with an inner volume of 110 µl (6 mm diameter, 4 mm and inner height) was coupled, connected to a syringe-driven flow pump. The functionalized sensor chips were mounted horizontally in the set up in order to prevent sedimentation of heavier components, causing possibly non-specific signals by physical adsorption. The sensor chip was hereby pressed mechanically onto the copper block. This block served as thermal reservoir and heat flow was generated using a thermistor on top of the copper block. The temperature of the copper, T_1, was measured by a thermocouple and actively steered through a PID controller (P = 8, I = 1, D = 0) which in turn was regulating the heating power. Throughout the measurement, this temperature was kept constant at 37.00 °C in order to

mimic body temperature and the ambient temperature remained constant at 19.0 °C. The temperature in the liquid, T_2, was measured with a second miniaturized thermocouple, positioned in the middle of the flow-through cell at a distance of 1.7 mm underneath the chip surface. The thermal resistance (R_{th}, given in °C/W) was then obtained by dividing the temperature difference ($T_1 - T_2$) through the input power P that is required to keep the copper block at the constant temperature $T_1 = 37.0\ ^0$C (Equation I). While the absolute value of R_{th} is governed mainly by the thermal conductivity of the buffer liquid, the positioning of the heated sensor chip at the top of the flow-through cell guarantees that there is no convection of liquid, which could possibly compromise the results.

$$R_{th} = \frac{T_1 - T_2}{P} \qquad \text{(I)}$$

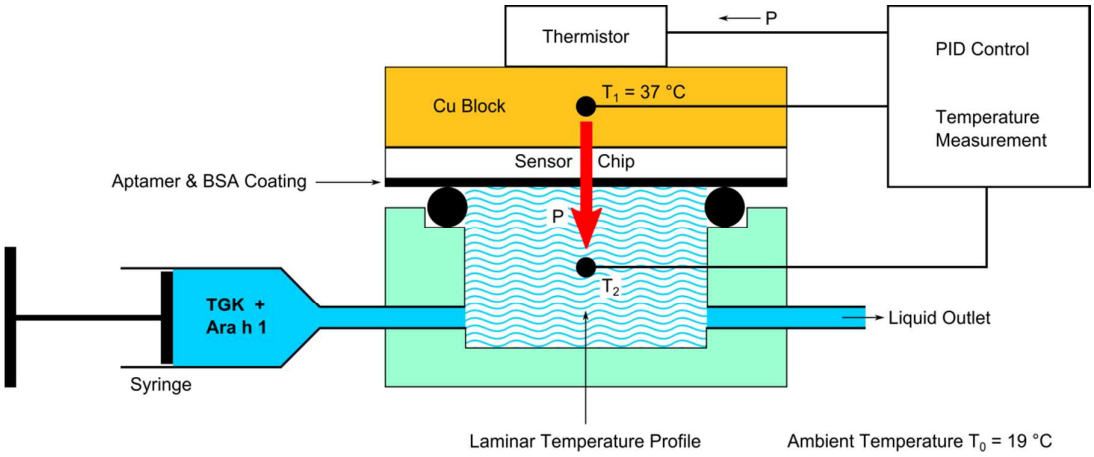

Figure 2: Schematic view of an aptamer-based setup for detecting changes of the thermal resistance upon molecular recognition of proteins. The thermal flow, generated by a thermistor, passes from the backside of the chip through the receptor layer into the sample liquid (heat-flow direction indicated by a red arrow). The temperature gradient is monitored using two thermocouples.

2.4 Microgravimetric measurements

Reference measurements with the quartz-crystal microbalance were performed on a QCM-D E4 system manufactured by Q-SENSE (Gothenburg, Sweden) and data were analyzed with QTools software. We employed UV-ozone treated gold-coated quartz crystals with a nominal

resonance frequency f_0 = 4.95 MHz and an active area size of 75 mm^2. One crystal was left blank, a second was activated with a self-assembled MUA-thiol linker layer and blocked with BSA, and the third chip received the full treatment with the linker layer, tethering of aptamers and finally blocked with BSA as well. All these steps were carried out according to the protocols given in Section 2.2. The measurement temperature (liquid and chip are here at an identical temperature) was 37 ^{0}C and we evaluated frequency shifts of the fundamental resonance frequency. Due to instrumental constraints, the QCM-sensor chips were mounted horizontally with the active coating facing upward towards the liquid sample.

1. Results and discussion

3.1 Thermal monitoring of aptamer functionalization

Prior to the actual protein-recognition experiment, we studied whether the tethering of the aptamers to the thiol-functionalized sensor chips would already bring about a measurable increase of the heat-transfer resistance R_{th}. In previous experiments with DNA sequences from exons of the PAH gene, it was observed that ds-DNA with up to 123 base pairs does not cause an R_{th} increase; this length is slightly below the persistence length of ds-DNA and the fragments are still considered as being 'mechanically quasi-stiff'. After denaturation to single-stranded fragments consisting of 123 bases, a clear R_{th} jump was observed and explained on grounds of the reduced persistence length of ss-DNA and curling up into Flory spheres[20,36].

In the present work, the immobilization of the 80-bases aptamer molecules was performed directly inside the HTM flow-through cell illustrated in Figure 2. First, a baseline was established by mounting a chip, comprising the thiol-linker layer, inside the cell and filling it up with MES buffer. Then, a solution containing MES buffer, aptamer molecules (0.1 μM), and EDC (400 mM) was added. The temperature T_1 was kept constant at 37.00 ^{0}C throughout the experiment. **Figure 3** presents the measured R_{th} values as bar charts normalized to a baseline defined by the heat-transfer resistance before addition of the aptamers and the EDC reagent. The baseline of 100% corresponds to an absolute value R_{th} of 8.01 ± 0.14 ^{0}C/W, determined by the materials, dimensions, and interfaces present along the heat-flow path between the two temperature sensors. The height of each bar in Figure 3 was determined as an averaged value over 1000 individual R_{th} data points, taken during a period of 1000 s with a sampling rate of 1 point per second. The width of the error bars is given by the standard deviation of the data with respect to the mean value within each of the five considered time intervals. Between 3000 s (50 minutes) and 4000 s (67 minutes) after addition

of the aptamer-EDC mixture, there is no significant change anymore in R_{th}, indicating that the reaction is completed. This duration of 60 minutes for an EDC-mediated linking reaction of amino-modified nucleotides to COOH groups is similar to the earlier reported optimal duration of approximately 2 hours[37]. This value of 2 hours was determined with a different monitoring technique (confocal fluorescence microscopy) and on polycrystalline diamond films, a chip material with a higher roughness than the gold layers employed within this study. Therefore, the 60 minutes for optimal EDC coupling found here are in line with the previous results of ref[38].

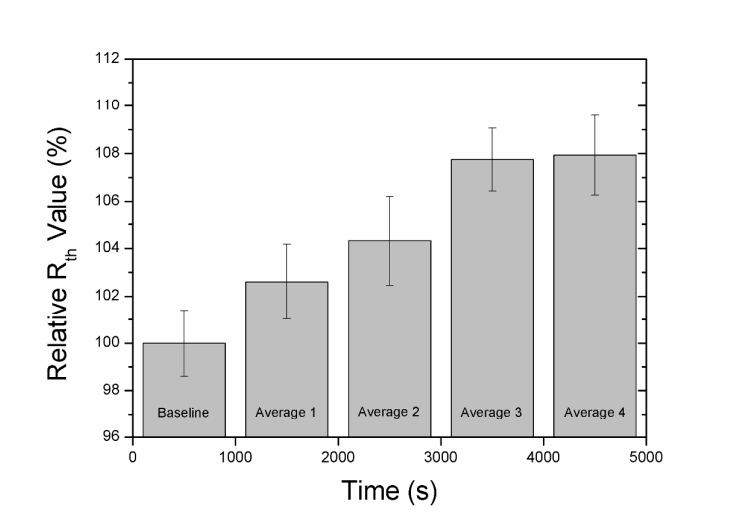

Figure 3: Relative increase of the heat-transfer resistance R_{th} during the EDC coupling of aptamers to the thiol-SAM linker layer. The baseline of 100% (corresponding to an absolute R_{th} = 8.0 ± 0.14 ^{0}C/W) was obtained during stabilization in MES buffer. A saturated aptamer coating increases the relative R_{th} to 108 ± 0.8 %. Each bar represents data averaged over a time interval of 1000 s.

The most important observation from Figure 3 is the fact that an aptamer monolayer displays a measurable R_{th} contribution (increase by 0.64 ^{0}C/W or 7.9 %). This is similar to single-stranded DNA, even quantitatively regarding the amplitude of the effect, and in contrast to double-stranded DNA where no measurable R_{th} increase occurs even for rather high areal densities of more than 10^{12} ds-fragments per cm^2 [20]. Correspondingly, it seems reasonable to assume that aptamers do have a mechanical flexibility irrespective of preferential folding such as indicated in Figure 1.

Next, one may assume that the adsorption of a BSA blocking layer should result in a second increase of the absolute R_{th} value: The adsorption process has to be performed at 4 ^{0}C in the refrigerator, meaning that it is not possible to monitor the BSA adsorption in real time because the HTM principle is only applicable when a temperature gradient is present. Instead, we performed a reference experiment with R_{th} monitoring at room temperature while the chip temperature was kept constant at $T_1 = 37.0$ ^{0}C. During the adsorption of BSA on a sensor chip covered with only the MUA SAM (no aptamer functionalization) we observed a minor R_{th} increase by 0.1 ± 0.05 ^{0}C. This increase stayed persistent even after rinsing and the data are given in the **Supporting Information,** Figure S2. This confirms the strong adhesive properties of BSA while its impact on the heat-transfer resistance is significantly less pronounced as compared to the aptamer.

3.2 *Thermal monitoring of protein recognition and reference testing*

After depositing the BSA overcoating, the sensor chip was installed again in the thermal-resistance setup (Figure 2) and the R_{th} measurement was started after filling the flow-through cell with TGK buffer and allowing stabilizing for 30 minutes. This initial stabilizing guarantees that the system is in thermal equilibrium. Then, Ara-h1 spiked TGK buffer was injected manually with increasing concentrations from 5 to 50 nM. Each spiked TGK sample had a volume of 1 ml, exceeding the inner volume of the flow-through cell 9 times. This way, we ensured that liquid from the previous concentration under study was fully removed from the flow-through cell and the tubing. **Figure 4A** shows a stepwise increase of the heat-transfer resistance for each next-higher concentration while the waiting time before adding the next-higher concentration was chosen 20 to 30 minutes. Immediately after injection of the next concentration there is a temporary overshooting of the R_{th} signal: This is an artifact due to the fact that the injected fluid is at room temperature, taking approximately 5 minutes to achieve again thermal-equilibrium conditions. Therefore, data obtained during the first 5 minutes for a given concentration are discarded. **Figure 4B** displays the concentration dependence of the normalized increase, reaching roughly 9 % for 50 nM of Ara h 1 in TGK. The width of the error bars represents the standard deviation on three separate measurements with the averaged value for a given concentration, ignoring data taken during the first five minutes after injection. For reference purposes, Figure 4B comprises also the normalized R_{th} data for the same Ara h 1 concentrations, but measured with a sensor chip without the aptamer functionality. All other chip features and handling, including the MUA-thiol SAM and the

BSA overcoating, are identical. Irrespective of the Ara-h 1 exposure, the R_{th} values measured with this reference chip remain constant within the error bars and only for the highest concentration (50 nM) one might infer a slight and non-specific R_{th} increase to 101 ± 0.8 %.

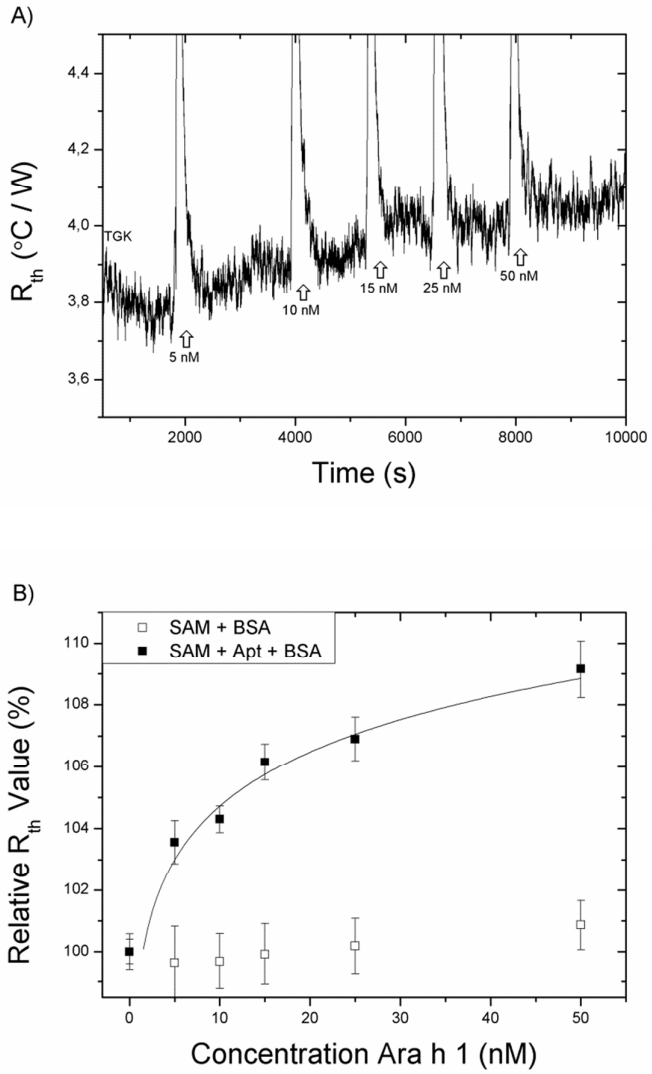

Figure 4: The upper panel (A) shows the absolute values of the heat-transfer resistance of the device with an aptamer-functionalized sensor chip for various concentrations of Ara h 1 in TGK buffer. The displayed data are non-smoothed, raw data. The lower panel (B) presents the data of panel A as solid boxes on a normalized scale with an allometric fit line according to Equation II. Error bars were calculated over three individual measurements with freshly prepared samples. The reference data given as open boxes were obtained with an identically

prepared sensor chip lacking the aptamer functionality. Within error bars, there is no indication for a false-positive response.

At this point it is verified that i) the protein recognition by aptamers enhances the interfacial heat-transfer resistance, ii) that the dose-response curve can give a quantitative information on the protein concentration, and iii) that the BSA overcoating has protein-repellant properties. The observation iii) is evident and expected from daily laboratory practice while i) and ii) are novelties and can thus be utilized as a new technique for label-free protein detection.
From Figure 4B we can now derive an estimate for the limit of detection LOD; the fit curve follows an allometric formula given by Equation II:

$$y = a \cdot x^{b} \qquad \text{(II)}$$

Here, x is the Ara h 1 concentration in nanoMolar units and y is the sensor response in % with 100 % corresponding to the baseline. The parameters of the fit curve are a = 99.1 %, b = 0.024 with a coefficient of determination $R^2 = 0.92$. The allometric fit describes the saturation effect occurring at high target molecules concentration and has been used before in ref[21,23].

The standard deviation of the signal at the lowest concentration (baseline) is 0.5 %. Defining the LOD as the concentration where the signal amplitude corresponds to the threefold standard deviation we estimate an LOD of 3 nM. The limit of quantification, corresponding to five times the standard deviation, is accordingly found at an Ara h 1 concentration of 4 nM. This agrees very well with the previously obtained value for aptamer-based Ara h 1 detection using impedance spectroscopy as readout technique[18]. For comparison, impedimetric protein sensors employing natural antibodies can still reach lower detection limits (< 1 nM), but antibodies are not really competitive with aptamers regarding their price, shelf-life, and reusability[39].

3.3 *Ara h 1 detection in peanut-butter extract*

First, a baseline was established in TGK buffer after which the peanut extract (50 mg of peanut butter in 200 ml TGK, see Section 2.2) was added and subsequently the extract that was additionally spiked with 100 nM of Ara h 1. The results are shown in **Figure 5** as bar charts for exposure times 30 min each, discarding data collected during the first 5 minutes

after injection. Upon exposing the functionalized sensor chip to the non-spiked peanut extract, a first increase by 2 ± 0.8 % was observed. By using the dose-response characteristics in buffer solutions according to Equation 2 this would correspond to an Ara h 1 concentration of ≈ 3 – 5 nM, thus below the maximum of 40 nM estimated from the protein content of the peanut butter. We point out that according to prior literature the Ara h 1 content decreases with increasing roasting time as compared to raw peanuts[34]. When the spiked solution (100 nM of Ara h 1) was introduced, the R_{th} value went further up to 111 ± 0.7 %. Assuming that the analytical form of the dose-response curve (Equation II) stays valid beyond the maximum concentration used for calibration, the increase to 111.3 % would correspond to an Ara h 1 concentration of 126 nM. This is in good agreement with the value of 100 nM from spiking plus native Ara h 1 present in the peanut butter.

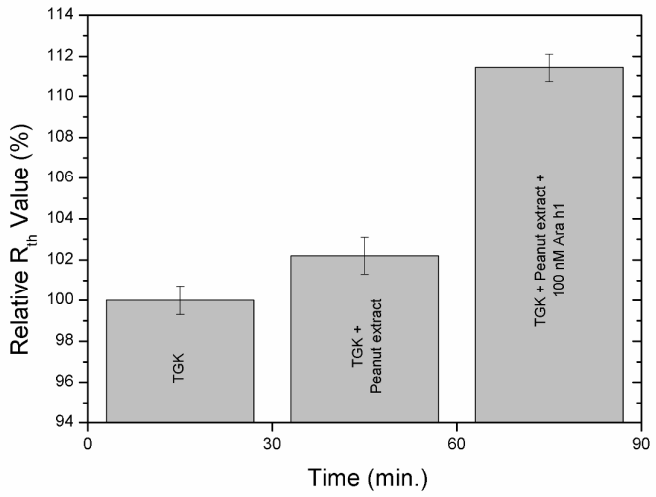

Figure 5: Measuring Ara h 1 in a peanut butter enriched matrix: The baseline was obtained in pure TGK buffer and the sample obtained from dissolved and filtrated peanut butter displays a measurable R_{th} increase by ± 2.2 %. The sample spiked with 100 nM of Ara h 1 (the total Ara-h1 contents slightly exceeds 100 nM) shows a substantial R_{th} increase by almost 12 % as compared to baseline level.

This is a first proof-of-application showing that screening of allergens can also be performed in liquefied and filtrated food samples. Furthermore, the magnitude of the R_{th} increase is surprisingly high comparing the size of the molecules that are bound to the solid-to-liquid interface to the overall macroscopic dimensions of the heat-flow path.

3.4 Comparative study with quartz-crystal microbalance QCM

Since the HTM-based results for protein detection are the first of their kind, additional control experiments were performed with the QCM, a well-established bioanalytical technique. For these experiments, we employed three Au-coated, standard QCM crystals: The first crystal was used as delivered with a non-modified gold surface, the second crystal was functionalized with a SAM-layer of MUA thiols and subsequently treated with a BSA blocking layer. The third crystal was functionalized with the SAM, followed by EDC linking of the aptamers, and finally overcoated with a BSA layer. All surface modifications were carried out according to the protocols given in Section 2.2 for the preparation of the HTM sensor chips. These references were used in order to verify the efficacy of the sensor coating independently and also to check for matrix-related viscosity effects due to the presence of peanut butter. Furthermore, there is a relevant difference with HTM because the functionalized quartz-crystals have to be mounted horizontally in the QCM device with the functionalized surface pointing upward. Therefore, the QCM data can in principle be affected by sedimentation of microparticles or heavier molecules. The experiment was conducted according to the same procedure as for the HTM experiments described in Section 3.3: First, the signal was stabilized in TGK buffer; thereafter, the non-spiked peanut extract was added, and finally the three different QCM chips were exposed to the peanut extract spiked with 100 nM of Ara h 1. The QCM-response of the three differently prepared quartz crystals to these three different solutions is summarized in **Figure 6**.

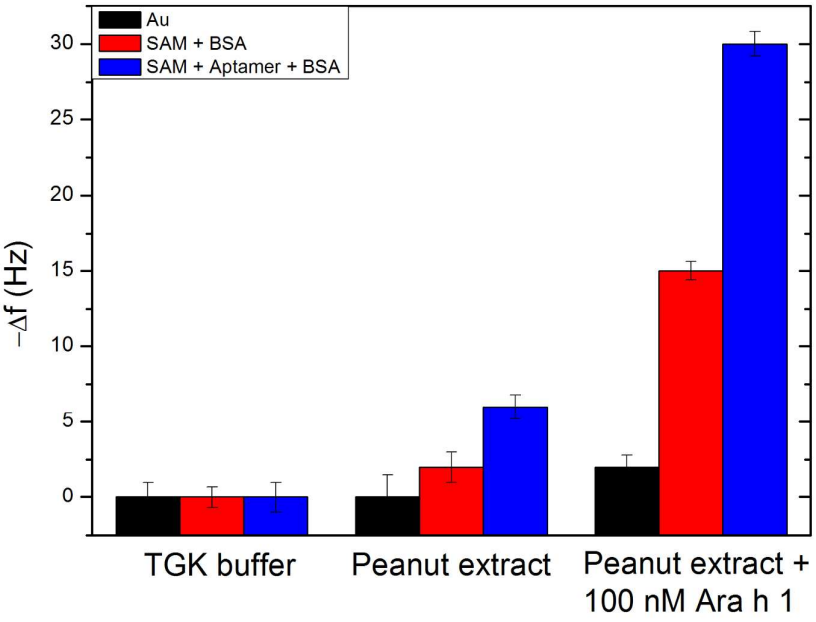

Figure 6: Shift of the resonance frequency Δf of the quartz crystals up exposure to pure TGK buffer (baseline), to the non-spike peanut extract, and to peanut extract spiked with 100 nM Ara h 1. The black bars correspond to non-treated quartz crystals with gold coating, the red bar represent crystals coated with the MUA, SAM and BSA, and the blue bars represent samples with MUA, SAM, aptamer functionalization and the BSA blocking layer.

The addition of the peanut extract or the extract spiked with Ara h 1 did not result in a significant frequency shift when the Au-coated QCM crystal was left non-functionalized. For the spiked sample we see a shift of 2 ± 1 Hz which is not there in case of the non-spiked extract. From this we can at least conclude that the measurements are not affected by the slightly enhanced viscosity of the extract as compared to pure TGK buffer. In case that the QCM crystals were treated with a SAM layer blocked with BSA, the crystal became more hydrophilic and was more prone to non-specific absorption. With only the peanut extract the increase was insignificant, but when spiked with 100 nM Ara h 1, a decrease by 15 ± 1 Hz was measured. This was however still significantly lower compared to the fully aptamer-functionalized crystal: In that case with the extract already a significant decrease by 6 ± 1 Hz was observed and with the spiked extract this resulted in a frequency drop by 30 ± 1 Hz. By taking the difference between the reference experiment (crystal with SAM and BSA, only

non-specific adsorption) and the sample functionalized with aptamer (non-specific adsorption and specific recognition together), the signal attributed to specific binding of Ara h 1 corresponds to 15 Hz. Here, we refer to the data obtained with the spiked extract and we not that the observed frequency shifts remained stable even after rinsing with TGK buffer.

If we assume that the Sauerbrey equation is valid, this frequency response equals a mass addition of roughly 204 ng or $6.2 \cdot 10^{11}$ specifically bound Ara h 1 molecules. Due to the high spiked Ara h 1 concentration we can furthermore assume that each of the tethered aptamer molecules captures one Ara h 1 protein. In combination with the active surface area of the QCM-sensor chips of 75 mm^2 we can deduce an areal density of approximately $8 \cdot 10^{11}$ bound aptamers per square centimeter. This is in the same order as the earlier determined surface density of double-stranded DNA fragments tethered to synthetic diamond layers with the fatty-acid & EDC coupling technique, being widely analogous with the protocol described in Section 2.2 [20,38]. Furthermore, we can give a rough estimate for the Flory radius r_F of an aptamer based on Equation III when ignoring for simplicity its self-folding properties[20]:

$$r_F \approx \sqrt{\frac{l_p \cdot L}{3}} \qquad \text{(III)}$$

The persistence length of single-stranded DNA is l_p = 1.5 nm and the fragment length is L = 28 nm for 85 bases. This results in a Flory radius $r_F \approx 3.7$ nm or $2.3 \cdot 10^{12}$ aptamers per cm^2, being approximately three times more than our indirect evaluation based on the QCM results.

The data illustrate that also QCM allows detecting Ara h 1 in a spiked but complex matrix. The QCM responds also to the non-spiked peanut extract; however the signal does not exceed the LOD defined by the threefold noise level and is partially due to non-specific adsorption effects. The adsorption effect is noticeable in the spiked- as well as in the non-spiked peanut extract which can be attributed to the horizontal configuration with the QCM chip underneath the fluid under study.

4. Conclusions

The heat-transfer method (HTM) monitors the properties at the solid-liquid interface and has been used in the past for the detection of cells, small organic molecules, and phase transition in lipids. We have shown for the first time the possibility to determine also protein

concentrations with this technique. This was demonstrated by employing an aptamer-based receptor system for the peanut protein Ara h 1. First, the functionalization procedure was followed *in situ*, confirming the presence of the aptamer on the gold surface, which had been pre-activated with a MUA-thiol linker layer. Then, proof-of-principle measurements were performed with Ara h 1 in buffer solutions. A dose-response curve was constructed up to Ara h 1 concentrations of 50 nM and the detection limit was in the order of ~ 3 nM, comparable to optimized values obtained by impedance spectroscopy. As a first proof-of-application, peanut extract and peanut extract spiked with Ara h 1 were studied, demonstrating the possibility to screen for trace allergens in liquefied and filtered food matrices. A distinguishable signal was already obtained with non-spiked peanut extract in which 50 mg of peanut butter was dissolved in a 20.000 times higher volume of TGK buffer.

To verify these results independently, additional experiments were conducted with the quartz-crystal microbalance QCM: Also this microgravimetric technique is capable of detecting Ara h 1 in a food matrix using aptamer receptors; however, it is considerably harder to integrate QCM in a miniaturized, portable and cost-efficient device. Nevertheless, the QCM experiments provided a very reasonable and realistic estimate for the areal density of aptamer receptors on gold surfaces in the order of $8 \cdot 10^{11}$ molecules per square centimeter. We point out that HTM requires especially little instrumental equipment while it can detect proteins specifically and label-free even in complex matrices. The combination of a blocking layer with an upside-down positioning of the sensor chip allowed to suppress non-specific adsorption to the widest possible extend. Moreover, the aptamers stayed at any time in their intrinsic conformation without necessitating the use of neutralizing oligomers, which are displaced upon binding of the target proteins. We assume that the described methodology offers a new approach for the quantitative detection of proteins including allergens and applications can be seen in biomedical- and clinical research as well as in food-safety screening.

Supporting Information Available

In the Supporting Information, a design with the exact dimensions of the heat-transfer resistance set up is provided and the effect on the thermal resistance when a BSA overcoating is applied onto the sample in order to minimize non-specific binding. Supporting information

to this document contains additional graphs that are referred to in the text. This material is available free of charge via the Internet at http://pubs.acs.org.

Author Information

Corresponding author

Dr. Marloes Peeters. Present address: Queen Mary University of London, Mile End Road, E14NS London, United Kingdom.
Phone: + 44 – 20 – 78 82 33 20, Email: m.peeters@qmul.ac.uk

Author Contributions

M.P. developed the recognition layer, prepared all samples and wrote the manuscript. The heat-transfer device was designed by B.v.G, and all heat-transfer measurements were performed by B.v.G. in cooperation with M.P. and T.C. B.v.G. and M.P. interpreted the heat-transfer data in close cooperation with W.D.C., R.T. and P.W.. K.L.J.M, P.C. and J.L assisted with the modeling of the aptamers and Ara h 1. E.R.P. provided the aptamers and assisted with questions regarding the immobilization protocols and conformational aspects. G.W. performed the heat-transfer measurements of the BSA overcoating. The manuscript was written by M.P. in collaboration with P.W. All authors have given approval to the final version of the manuscript.

Acknowledgements: This work is supported by the Research Foundation Flanders FWO (project G.0997.11N), the Life Science Initiative of the Belgian Province of Limburg and the European Commission's Seventh Framework Program (FP7/2007-2013) under the grant agreement BIOMAX (Project No. 264737). The authors also would like to thank H. Penxten, J. Soogen, C. Willems, J. Baccus, and P. Robaeys for technical assistance as well as M. Khorshid and M. Dollt for providing the heat-transport data on BSA coatings.

References

[1] Hermann, T. and Patel, D.J. Adaptive Recognition by Nucleic Acid Aptamers, *Science* **2000,** 287, 820 – 825.

[2] Brody. E.N. and Gold, L. Aptamers as Therapeutic and Diagnostic Agents, *Rev. Mol. Biotechnol.* **2000,** 74, 5 – 13.

[3] Fang, X. and Tan, W. Aptamers Generated from Cell-SELEX for Molecular Medicine : A Chemical Biology Approach, *Acc. Chem. Res.* **2010,** 43, 48 – 57.

[4] Stoltenburg, R.; Reinemann, C.; Strehlitz, B. FluMag-SELEX as an Advantageous Method for DNA Aptamer Selection, *Anal. Bioanal. Chem.* **2005,** 383, 83 – 91.

[5] Li, L.; Li, B.; Qi, Y.; Jin, Y.; Label-free Aptamer-based Colorimetric Detection of Mercury Ions in Aqueous Media using unmodified Gold Nanoparticles as Colorimetric Probe, *Anal. Bioanal. Chem.* **2009,** 393, 2051 – 2057.

[6] Maehashi, K.; Katsura, T.; Kerman, K.; Takamura, Y.; Matsumoto, K.; Tamiya, E.; Label-free Protein Biosensor based on Aptamer-modified Carbon Nanotube Field-effect Transistors, *Anal. Chem.* **2007,** 79, 782 – 787.

[7] Ikebukuro, K.; Kiyohara, C.; Sode, K. Novel Electrochemical Sensor System for Proteins using the Aptamers in Sandwich Manner, *Biosens. Bioelectron.* **2005,** 20, 2168 – 2172.

[8] Shangguan, D.; Meng, L.; Cao, Z.C.; Xiao, Z.; Fang, X.; Li, Y.; Cardona, D.; Witek, R.P.; Liu, C.; Tan, W. Identification of Liver Cancer-specific Aptamers using Whole Live Cells, *Anal. Chem.* **2008,** 80, 721 – 728.

[9] Tang, Z.; Shangguan, D.; Wang, K.; Shi, H.; Sefah, K.; Mallikratchy, P.; Chen, H.W.; Li, Y.; Tan, W. Selection of Aptamers for Molecular Recognition and Characterization of Cancer Cells, *Anal. Chem.* **2007,** 79, 4900 – 4907.

[10] Buchanan, D.D.; Jameson, E.E.; Perlette, J.; Malik, A.; Kennedy, R.T. Effect of Buffer, Electric Field, and Separation Time on Detection of Aptamer-Ligand Complexes for Affinity Probe Capillary Electrophoresis, *Electrophoresis* **2003,** 24, 1375-1382.

[11] Liu, J. and Lu, Y. Fast Colorimetric Sensing of Adenosine and Cocaine Based on General Sensor Design Involving Aptamers and Nanoparticles, *Angew. Chem., Int. Ed.* **2005,** 118, 96 – 100.

[12] Fang, X. Cao, Z.; Beck, T.; Tan, W. Molecular Aptamer for Real-time Oncoprotein Platelet-derived Growth Factor Monitoring by Fluorescence Anistropy, *Anal. Chem.* **2001,** 73, 5752 – 5757.

[13] Tran, D.T.; Knez, K.; Janssen, K.P.F.; Pollet, J.; Spasic, D.; Lammertyn, J. Selection of Aptamers against Ara h 1 Protein for FO-SPR Biosensing of Peanut Allergens in Food Matrices, *Biosens. Bioelectron.* **2013,** 43, 245 – 251.

[14] Yao, C.; Zhu, T.; Qi, Y.; Zhao, Y.; Xia, H.; Fu, W. Development of a Quartz Crystal Microbalance Biosensor with Aptamers as Bio-recognition Element, *Sensors* **2010,** 10, 5859 – 5871.

[15] Rodriguez, M.C.; Kawde, A.N.; Wang, J. Aptamer Biosensor for Label-free Impedance Spectroscopy Detection of Proteins based on Recognition-induced Switching of the Surface Charge, *Chem. Commun.* **2005,** 14, 4267 – 4269.

[16] Cai, H.; Lee, T.M.-H.; Hsing, I.-M. Label-free Protein Recognition using an Aptamer-based Impedance Measurement Array, *Sens. Actuators, B.* **2006,** 114, 433 – 437.

[17] Goda, T. and Miyahara, Y. Label-free and Reagent-less Protein Biosensing using Aptamer-modified Extended Gate Field-effect Transistors, *Biosens. Bioelectron.* **2013,** 45, 89 – 94.

[18] Tran, D.T.; Vermeeren, V.; Grieten, L.; Wenmackers, S.; Wagner, P.; Pollet, J.; Janssen, K.P.F.; Michiels, L.; Lammertyn, J. Nanocrystalline Diamond Impedimetric Aptasensor for the Label-free Detection of Human IgE, *Biosens. Bioelectron.* **2011,** 26, 2987 – 2993.

[19] Peeters, M.; Jiménez-Monroy, K.L.; Libert, C.; Eurlings, Y.; Cuypers, W.; Wackers, G.; Duchateau, S.; Robaeys, P.; Nesládek, M.; van Grinsven, B.; Pérez-Ruiz, E.; Lammertyn, J.;. Losada-Pérez, P.; Wagner, P.; Real-Time Monitoring of Aptamer Functionalization and Detection of Ara h 1 by Electrochemical Impedance Spectroscopy and Dissipation-Mode Quartz Crystal Microbalance, *J. Biosens. Bioelectron.* **2014,** 5, DOI: 10.4172/2155-6210.1000155.

[20] van Grinsven, B.; Vanden Bon, N.; Strauven, H.; Grieten, L.; Murib, M.; Jiménez-Monroy, K.L.; Janssens, S.D.; Haenen, K.; Schöning, M.J.; Vermeeren, V.; Ameloot,M.; Michiels, L.; Thoelen, R.; De Ceuninck, W.; Wagner, P. Heat-Transfer Resistance at Solid-Liquid Interfaces: A Tool for the Detection of Single-Nucleotide Polymorphisms in DNA, *ACS Nano* **2012,** 6, 2712 – 2721.

[21] van Grinsven, B.; Eersels, K.; Peeters, M.; Losada-Pérez, P.; Vandenryt, T.; Cleij, T.J.; Wagner, P. The Heat-Transfer Method: A Versatile, Low-Cost, Label-free, and User-friendly Readout Platofrm for Biosensor Applications, *ACS Appl. Mater. Interfaces* **2014,** 6, 13309 – 13318.

[22] Bers, K.; Eersels, K.; van Grinsven, B.; Daemen, M.; Bogie, J.; Hendriks, J.; Bouwmans, E.; Püttmann, C.; Stein, C.; Barth, S.; Bos, G.; Germeraad, W.; De Ceuninck, W.; Wagner, P. Heat-Transfer Resistance Measurement Method (HTM)-Based Cell Detection at Trace Levels Using a Progressive Enrichment Approach with Higly Selective Cell-Binding Surface Imprints, *Langmuir* **2014,** 30, 3631 – 3639.

[23] Peeters, M.; Csipai, P.; Geerets, B.; Weustenraed, A.; van Grinsven, B.; Gruber, J.; De Ceuninck, W.; Cleij, T.J.; Troost, F.J.; and Wagner, P. Heat-Transfer-Based Detection of L-Nicotine, Histamine, and Serotonin Using Molecularly Imprinted Polymers as Biomimetic Receptors, *Anal. Bioanal. Chem.* **2013,** 405, 6453 – 6460.

[24] Losada-Pérez, P.; Jiménez-Monroy, K.L.; van Grinsven, B.; Leys, J.; Janssens, S.D.; Peeters, M.; Glorieux, C.; Thoen, J.; Haenen, K.; De Ceuninck, W.; Wagner, P. Phase Transitions in Lipid Vesicles Detected by a Complementary Set of Methods: Heat-Transfer Measurements, Adiabatic Scanning Calorimetry, and Dissipation-Mode Quartz Crystal Microbalance, *Phys. Status Solidi A* **2014,** 211, 1377 – 1388.

[25] Wang, C.; Hossain, M.; Ma, L.; Ma, Z.; Hickman, J.J.; Su, M. Highly Sensitive Thermal Detection of Thrombin Using Aptamer-Functionalized Phase Change Materials, *Biosens. Bioelectron.* **2010,** 26, 437 – 443.

[26] Velizhanin, K.A.; Chien, C.-C. Dubi, Y.; Zwolak, M. Driving Denaturation: Nanoscale Thermal Transport as a Probe of DNA Melting, *Phys. Rev. E: Stat., Nonlinear, Soft Matter Phys.* **2011,** 83, 1-4.

[27] Nakano, T.; Kikugawa, G.; Ohara, T. A Molecular Dynamics Study on Heat Conduction Characteristics in DPPC Lipid Bilayer, *J. Chem. Phys.* **2010,** 133, 154705-154714.

[28] Eersels, K.; van Grinsven, B.; Ethirajan, A.; Timmermans, S.; Jiménez-Monroy, K.L.; Bogie, J.F.J.; Punniyakoti, S.; Vandenryt, T.; Hendriks, J.J.A.; Cleij, T.J.; Daemen, M.J.A.P.; Somers, V.; De Ceuninck, W.; Wagner, P. Selective Indentification of Macrophages and Cancer Cells Based on Thermal Transport Through Surface-Imprinted Polymer Layers, *ACS Appl. Mater. Interfaces*, **2013,** 5, 7258-7267.

[29] Das, J. Cederquist, K.B.; Zaragoza, A.A.; Lee, P.E.; Sargent, E.H.; Kelly, S.O. An Ultrasensitive Universal Detector Based on Neutralizer Displacement, *Nat. Chem.* **2012,** 4, 642 – 648.

[30] Pérez-Ruiz, E.; Kemper, M.; Spasic, D.; Gils, A.; van IJzendoorn, L.; Lammertyn, J.; Prins, M.W.J. Probing the Force-Induced Dissociation of Aptamer-Protein Complexes, *Anal. Chem.* **2014,** 86, 3084 – 3091.

[31] Zuker, M. Mfold web server for Nucleic Acid Folding and Hybridization Prediction, *Nucleic Acids Res.*, **2003,** 31, 3406 – 3415.

[32] Maleki, S.J.; Kopper, R.A.; Shin, D.S.; Park, C-W.; Compadre, C.M.; Sampson, H.; Burks, A.W.; Bannon, G.A. Structure of the Major Peanut Allergen Ara h 1 May Protect IgE-binding Epitopes from Degradation, *J. Immunol.*, **2000,** 164, 5844 – 5849.

[33] Jeyachandran, Y.L.; Mielczarski, E.; Rai, B.; Mielczarski, J.A. Quantitive and Qualitative Evaluation of Adsorption/Desorption of Bovine Serum Albumin on Hydrophilic and Hydrophobic Surfaces, *Langmuir,* **2009,** 25, 11614 – 11620.

[34] Pomés, A.; Butts, C.L.; Chapman, M.D. Quantifcation of Ara h 1 in peanuts : Why Roasting Makes a Difference, *Clin. Exp. Allergy,* **2006,** 36, 824 – 830.

[35] Ogasawara, D.; Hachiya, N.S.; Kaneko, K.; Sode, K.; Ikebukuro, K. Detection System Based on the Conformational Change in an Aptamer and its Application to Simple Bound/Free Separation, *Biosens. Bioelectron.* **2009,** 24, 1372 – 1376.

[36] Vanden Bon, N.; van Grinsven, B.; Murib, M.S.; Yeap, W.S.; Haenen, K.; De Ceuninck, W.; Wagner, P.; Ameloot, M.; Vermeeren, V.; Michiels, L. Heat-Transfer Based Detection of SNPS in the PAH Gene of PKU Patients, *Int. J. Nanomed.* **2014,** 9, 1629 – 1640.

[37] Jhaveri, S.D.; Kirby, R.; Conrad, R.; Maglott, E.J.; Bowser, M.; Kennedy, R.T.; Glick, G.; Ellington, A.D. Designed Signaling Aptamers that Transduce Molecular Recognitions Changes in Fluorescence Intensity, *J. Am. Chem. Soc.* **2000,** 122, 2469 – 2473.

[38] Vermeeren, V.; Wenmackers, S.; Daenen, M.; Haenen, K.; Williams, O.A.; Ameloot, M.; vandeVen, M.; Wagner, P.; Michiels, L. Topographical and Functional Characterisation of the ssDNA Probe Layer Generated Through EDC-mediated Covalent Attachment to Nanocrystalline Diamond Using Fluorescence Microscopy, *Langmuir,* **2008,** 24, 9125 – 9134.

[39] Trashin, S.; De Jong, M.; Breugelmans, T.; Pilehvar, S.; De Wael, K. Label-Free Impedance Aptasensor for the Major Peanut Allergen Ara h 1, *Electroanalysis,* **2015,** 27**,** 32-37.

Figure Table of Content: